Proposed Mechanism for the Biosynthesis of the [FeFe] Hydrogenase H-Cluster: Central Roles for the Radical SAM Enzymes HydG and HydE

R. David Britt,* Lizhi Tao, Guodong Rao, Nanhao Chen, and Lee-Ping Wang

Read Online

ACCESS | Metrics & More | Article Recommendations

ABSTRACT: Radical *S*-adenosylmethionine (radical SAM or rSAM) enzymes use their *S*-adenosylmethionine cofactor bound to a unique Fe of a [4Fe−4S] cluster to generate the "hot" 5′-deoxyadenosyl radical, which drives highly selective radical reactions via specific interactions with a given rSAM enzyme's substrate. This Perspective focuses on the two rSAM enzymes involved in the biosynthesis of the organometallic H-cluster of [FeFe] hydrogenases. We present here a detailed sequential model initiated by HydG, which lyses a tyrosine substrate via a 5′-deoxyadenosyl H atom abstraction from those amino acid's amino group, initially producing dehydroglycine and an oxidobenzyl radical. In this model, two successive radical cascade reactions lead ultimately to the formation of HydG's product, a mononuclear Fe organometallic complex: $[Fe(II)(CN)(CO)_2(cysteinate)]^-$, with the iron originating from a unique "dangler" Fe coordinated by a cysteine ligand providing a sulfur bridge to another [4Fe−4S] auxiliary cluster in the enzyme. In turn, in this model, $[Fe(II)(CN)(CO)_2(cysteinate)]^-$ is the substrate for HydE, the second rSAM enzyme in the biosynthetic pathway, which activates this mononuclear organometallic unit for dimerization, forming a $[Fe_2S_2(CO)_4(CN)_2]$ precursor to the $[2Fe]_H$ component of the H-cluster, requiring only the completion of the bridging azadithiolate (SCH_2NHCH_2S) ligand. This model is built upon a foundation of data that incorporates cell-free synthesis, isotope sensitive spectroscopies, and the selective use of synthetic complexes substituting for intermediates in the enzymatic "assembly line". We discuss controversies pertaining to this model and some remaining open issues to be addressed by future work.

KEYWORDS: Cell free synthesis, isotope editing, pulse EPR, ENDOR, HYSCORE

Mechanistic study of radical SAM enzymes
■ cell-free biosynthesis
■ isotope sensitive spectroscopy
■ synthetic complexes

H-cluster, $[2Fe]_H$
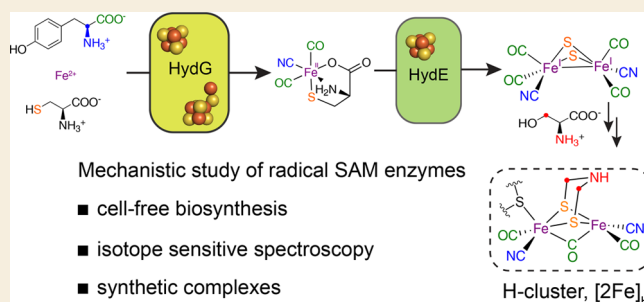
INTRODUCTION

As extensively discussed in this special issue of *ACS Bio & Med Chem Au*, radical *S*-adenosylmethionine (radical SAM or rSAM) enzymes play a variety of key roles in biochemistry, with one important subclass being the synthesis of complex catalytic metal clusters of metalloenzymes such as nitrogenases and hydrogenases.[1−3] We have focused much of our recent efforts on the radical SAM enzymes involved in key steps in the biosynthesis of the "H-cluster" of the [FeFe] hydrogenases, which catalyzes the redox interconversion of protons and electrons with molecular hydrogen. The [FeFe] hydrogenases (there are also [NiFe] and Fe-only hydrogenases) are well suited to H_2 formation, producing up to 10 000 H_2 molecules per second, and have therefore generated much interest for renewable energy applications.[4−8] The H-cluster consists of a binuclear $[2Fe]_H$ subcluster which is linked via a bridging cysteine to a [4Fe−4S] cluster ($[4Fe]_H$) (Figure 1). This $[2Fe]_H$ subcluster contains the organometallic elements of the H-cluster: the two irons each have a CO and a CN^- terminal ligand and are bridged by a third CO and a unique

SCH_2NHCH_2S azadithiolate (adt) moiety (Figure 1). The H^+ and H_2 substrates are proposed to bind to and react at this $[2Fe]_H$ unit.[8−12] In addition to the relative rarity of enzymes carrying out organometallic reactions, the biosynthesis of the H-cluster poses some specific challenges. Of course, free CO and CN^- molecules are toxic. In addition, the bridging adt moiety is known to be unstable in solution.[13]

The $[2Fe]_H$ subcluster is synthesized and linked to the $[4Fe]_H$ subcluster to form the active H-cluster (Figure 1) by a set of three Fe−S proteins, HydE, HydF, and HydG.[15−24] Two members of this set of "maturase" proteins, HydE and HydG, are radical SAM enzymes.
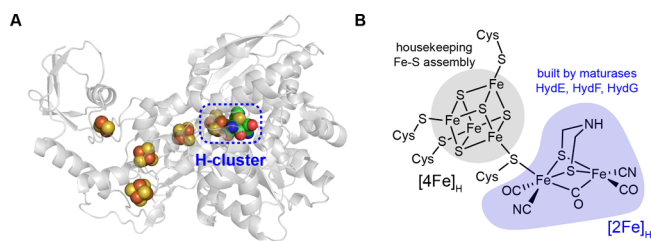
Figure 1. [FeFe] hydrogenase and its active site. (A) Crystal structure of *Clostridium pasteurianum* CpI (PDB ID: 4XDC) highlighting the H-cluster and accessory Fe–S clusters serving as electron transfer wires. (B) Structure of the catalytic H-cluster, with the subclusters $[4Fe]_H$ and $[2Fe]_H$ that are assembled by different pathways. Reproduced from ref 14 with permission from the Royal Society of Chemistry.

After a brief historical review (for a more complete historical discussion, please see ref 14), we begin this Perspective by discussing how magnetic isotopes and chemical labels have been used to determine the molecular origins of all of the elements of the H-cluster.[3] We have also used such isotopes and chemical labels to follow the reactions of the individual maturase enzymes, where the recent evidence points to a sequential mechanism, in order of enzymes HydG to HydE to HydF (Figure 2). Through the use of time-resolved spectros-
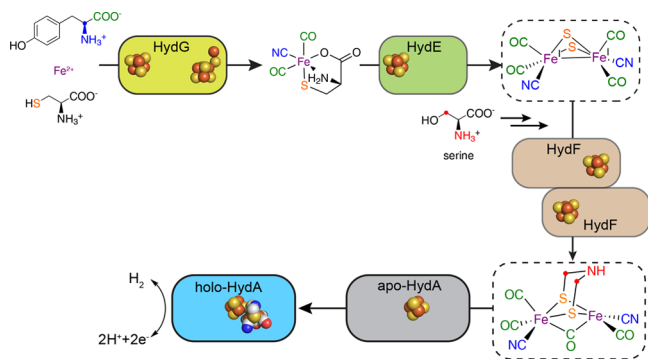

Figure 2. Sequential model for the roles of the HydG, HydE, and HydF maturases in the biosynthesis of the [FeFe] hydrogenase H-cluster along with the molecular sourcing of each atom in the $[2Fe]_H$ subcluster. Reproduced from ref 14 with permission from the Royal Society of Chemistry.

copies, supplemented by quantum chemical calculations, we have developed a detailed mechanistic model for the biosynthesis of the H-cluster. A presentation of this model along with its supporting data is the primary focus of this Perspective.

■ BRIEF HISTORY OF THE Fe–S MATURASES

[FeFe] hydrogenases have been naturally found in numerous anaerobic microorganisms and green algae. The most widely studied [FeFe] hydrogenases, on which early crystallographic studies were performed, were those naturally purified from the nitrogen-fixing bacterium *Clostridium pasterianum*, the sulfate-reducing bacterium *Desulfovibrio desulfuricans*, as well as the green algae *Chlamydomonas reinhardtii* homologue hetero-logously expressed in *Escherichia coli*.[25] It was later discovered by Posewitz *et al.*,[15] in a genetics/molecular biology study, that three genes, *hydE*, *hydF*, and *hydG*, play essential roles in H-cluster synthesis. Subsequently, the *hydE*, *hydF*, and *hydG*

genes from *Clostridium acetobutylicum* and *Shewanella oneidensis* have been frequently used to heterologously synthesize the H-cluster in vivo or in vitro. Coexpression of these genes along with the hydrogenase *hydA1* gene provided a new ability to produce active HydA1 hydrogenase via heterologous expression. For example, *E. coli* with only the *hydA1* gene added produces only the $[4Fe-4S]_H$ component of the H-cluster (Figure 1).[20] McGlynn et al.[18] showed that inactive HydA expressed in *E. coli* was rapidly converted to active enzyme by the addition of a protein extract with HydE, HydF, and HydG expressed in concert. Kuchenreuther et al.[26] carried out the in vitro maturation of [FeFe] hydrogenase HydA1 protein using individually expressed and purified HydE, HydF, and HydG. This innovation allowed them to determine how each maturase affects the kinetics of hydrogenase activation. Interestingly, under these maturation conditions, including a cocktail of small molecule additives plus *E. coli* cell lysate, only HydG was absolutely required for the assembly of active hydrogenase, whereas without HydE or HydF the activation was found to be incomplete, resulting in low hydrogenase activity.

In a separate and dramatic development, it was also shown that a synthetic precursor of the $[2Fe]_H$ complex, $[(Fe_2(adt)-(CN)_2(CO)_4]^{2-}$, can be integrated with the $[4Fe-4S]_H$ -only cluster form of HydA1 to generate a highly active H-cluster. Artificial maturation was first demonstrated with HydF included in the reaction mix,[27] but it was soon shown that even HydF was not needed.[28] These "semisynthesis" studies directly reinforce the picture that the three maturases are required for building the natural $[2Fe]_H$ subcluster, since they can all be deleted if the appropriate synthetic analogue is instead provided. One detail that proves relevant subsequently, is that the product of the three maturases is a $(CO)_4$ complex, whereas the HydA requires the $(CO)_3$ derivative. Thus, the maturases appears to produce a CO-inhibited form of the enzyme. In addition, the artificial maturation has been applied to the synthesis of myriad modifications of the active site.[29,30]

In order to understand the mechanism of H-cluster biosynthesis, it is important to characterize the role played by each of these three Fe–S maturases. HydG has a high sequence homology with ThiH,[31] a rSAM enzyme that lyses L-tyrosine to generate dehydroglycine (DHG) and *p*-cresol. Pilet et al.[21] showed that HydG SAM cleavage is stimulated by tyrosine and identified *p*-cresol as a product in analogy to ThiH. Driesener et al.[22] demonstrated that HydG produces cyanide from tyrosine, and Shepard et al.[23] showed that HydG produces CO as well (as measured by CO binding to external deoxyhemoglobin). Thus, in general, HydG forms the CO and CN^- ligands of the $[2Fe]_H$ subcluster via a rSAM-based radical interaction with its tyrosine substrate. It was then proposed that the other rSAM enzyme HydE is responsible for the synthesis of the adt bridge.[23,32] With the model that the adt bridge and CO and CN^- are produced by the two rSAM enzymes, it was proposed that these assemble onto an existing [2Fe–2S] cluster on HydF to complete the $[2Fe]_H$ subcluster before transferring it to HydA1 for completion of the full H-cluster.[23,32−34]

It is important also to note that although the [FeFe] and [NiFe] hydrogenases carry out parallel reactions and have some corresponding organometallic structural elements, the [NiFe] center is biosynthesized without any radical SAM enzymes. Thus, in this Perspective, we do not discuss its biosynthesis further but refer the interested reader to our

recent review comparing the two distinct assembly mechanisms (as well as that of the nitrogenase cofactor).[3]

THE MOLECULAR SOURCING OF THE INDIVIDUAL ELEMENTS OF THE $[2Fe]_H$ CLUSTER

The in vitro maturation (or cell free synthesis) approach allows one to directly introduce magnetic nuclear isotopes via substrates and cofactors that feed into the H-cluster assembly.[26] By introducing these in the cocktail of ingredients needed to enable these in vitro assembly reactions, we avoid possible side reactions and isotopic scrambling that could occur during in vivo cellular metabolism. In addition, the quantity of expensive labeled isotopes is lowered significantly by this route. Combined with continuous wave EPR and high resolution pulse EPR methods, this allows one to determine the source of the individual atoms of the H-cluster, as measured in the various paramagnetic H-cluster forms such as H_{ox}, $H_{ox}CO$, and H_{hyd}.[3,35−37] Other isotope sensitive spectroscopies such as FTIR and Mössbauer (specifically for ^{57}Fe)[38] can provide such information for H-cluster states regardless of whether they are EPR active, as can EXAFS for sulfur to selenium substitution.[39] Figure 2 summarizes the assigned molecular sourcing obtained by such methods. As noted before, the CN^- and CO ligands are sourced from tyrosine, which is the substrate of the radical SAM chemistry of HydG. These results also show that the Fe and S atoms that form the Fe_2S_2 core of the $[2Fe]_H$ also come from HydG via its product "synthon", a $[Fe(CN)(CO)_2(cysteinate)]^-$ organometallic complex (vide infra). Notably, the only components that are not sourced from this HydG product are the CH_2NHCH_2 components of the adt bridge, which instead originate from the 3-C and amino-N of serine.[40]

A SEQUENTIAL MECHANISTIC PROPOSAL FOR H-CLUSTER ASSEMBLY

As noted, Figure 2 presents our proposed sequence of enzyme action among the three maturase enzymes, along with molecular sources for all of the elements of the $[2Fe]_H$ subcluster as incorporated into the fully active H-cluster. Using the same combination of magnetic isotopes and chemical modifications, including incorporation into molecular precursors inserted into semisynthetic H-cluster assembly, we have developed the detailed mechanistic model shown in Figure 3. Here we have used isotope sensitive spectroscopies and mass spectrometry to probe intermediates of the maturase reactions in addition to their products. Not only does this give us structural information about the intermediates, but this approach also provides details of the underlying kinetics. This provides a strong basis for a quantum chemistry approach to further analysis electronic structures and energetics of intermediates, as well as to interpolate between experimentally determined structures to suggest heretofore unknown reaction intermediates. Figure 3 provides a block diagram of the overall proposed mechanisms as a set of interlinked sequential reaction modules, rather like subassembly stations of an automobile assembly line, which involves transfer of components from one reaction/assembly site to the next. Thus, this sequential assembly model is very different from the initial model of Shepard and co-workers[23,32−34] for H-cluster assembly, in which the parts are all assembled "in parallel" with the final assembly occurring at one station.
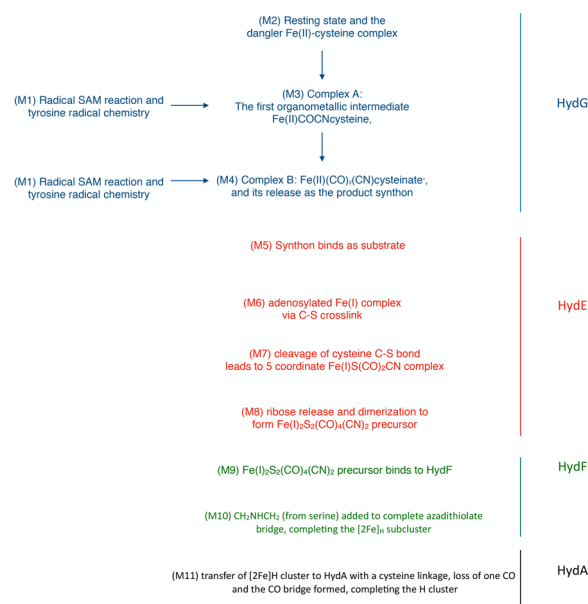

Figure 3. Block diagram overview off the modules (M1−M11) that compose the sequential H-cluster biosynthesis model. Fe(I) and Fe(II) denote the oxidation number of iron for each intermediate.

Each of the modules in this block diagram is detailed in the following sections, organized by the relevant enzyme, in the sequence HydG to HydE to HydF.

HydG

A breakthrough in our understanding of HydG came with the 2015 *Thermoanaerobacter italicus* (*Ti*) HydG structure (Figure 4) by Dinis et al.[41] In addition to the previously suspected
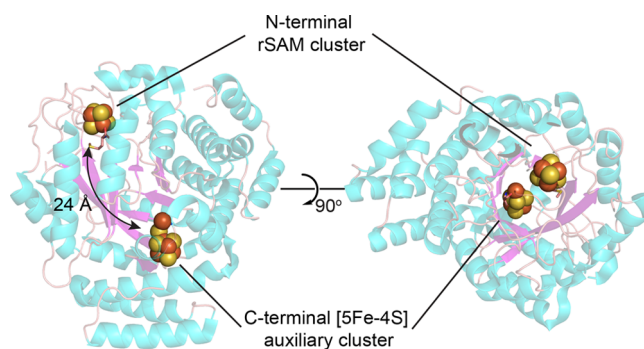

Figure 4. Crystal structure of *Thermoanaerobacter italicus* (*Ti*) (PDB ID: 4WCX). The two Fe−S clusters in HydG are located at each end of an ≈24 Å TIM-barrel channel (magenta).[41] Reproduced from ref 14 with permission from the Royal Society of Chemistry.

radical SAM $[4Fe−4S]$ cluster, the crystal structure revealed the presence of an additional $[4Fe−4S]$ cluster bridged to a fifth "dangler Fe". The two FeS clusters are connected by an ≈24 Å TIM (triosephosphate isomerase) barrel channel made of eight α-helices and eight parallel β-strands. In the proposed sequential mechanism described here, HydG plays a bifunctional role, with interesting reactions assigned at each cluster and in a rational temporal sequence based on both the separation of the two clusters and their innate connectivity via the TIM barrel channel.
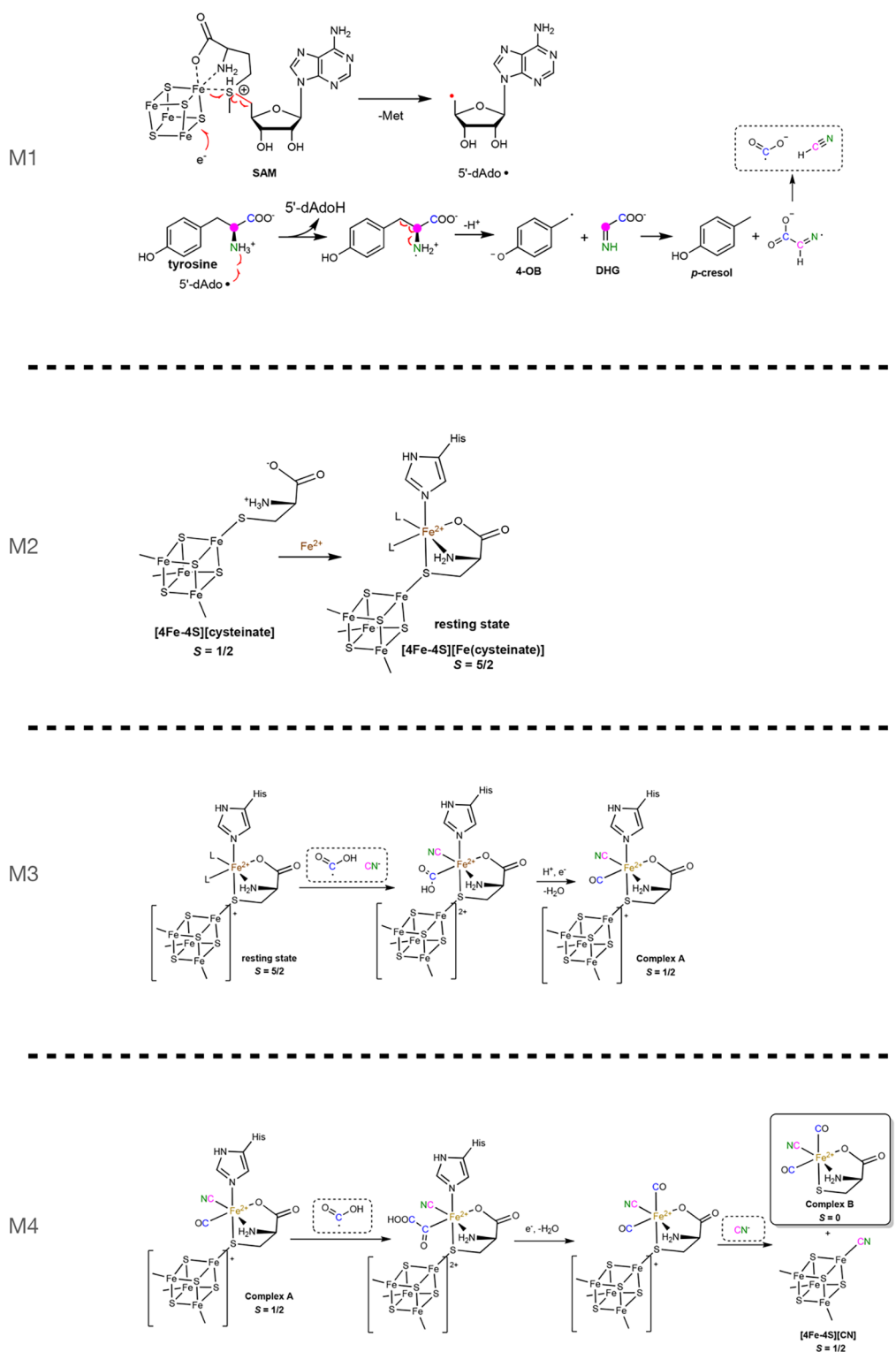
Figure 5. Detailed reaction modules (M1−M4) of the radical SAM enzyme HydG.

Module 1: Tyrosine Lysis

Evidence: X-ray Crystal Structures, EPR Spectroscopy, Reactivity of Tyrosine Analogues, and Quantum Chemistry (See Figure 5 M1). The *Ti*HydG structure shows canonical SAM binding to the [4Fe−4S] cluster (in one of two monomers in the unit cell).[41] The substrate tyrosine is not found in the structure, but it was instead modeled into the crystal structure based on the structure of a homologous rSAM

tryptophan lyase, NosL, that revealed the binding site for tryptophan.[42] Also, in the nosL structure, the tryptophan substrate is oriented so as to facilitate 5′dAdo• H atom abstraction from the amino group of the tryptophan, and the authors suggested that a similar amino H atom abstraction drives the tyrosine fragmentation in HydG and other tyrosine lyases.[42] We used EPR of samples "rapid freeze quenched (RFQ)" after reaction initiation to search for observed radical

intermediates, and the use of a variety of tyrosine isotopologs was key to the assignment of a trapped 4-oxidobenzyl (4-OB$^\bullet$) radical whose EPR intensity was maximal following a few seconds of the reaction (Figure 6).[43] Sayler et al.[44] studied the
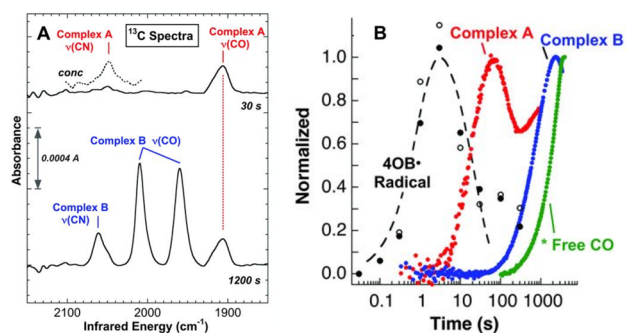

Figure 6. FTIR spectra. Reactions used 100 μM *So*HydG^{WT} (unless noted) and ^{13}C$_9$-Tyr, producing ^{13}C O and ^{13}C N ligands. (A) SF-FTIR spectra measured at 30 and 1200 s (solid lines) and at 10 s using 800 μM HydG^{WT} (dotted line, plotted at half intensity). (B) Time dependence of formation and decay of the following species: 4OB$^\bullet$ determined by EPR spectroscopy, two experimental runs and corresponding kinetic fit (dashed line);[43] FTIR data of Complex A (red) and Complex B (blue) determined by the peak heights of their respective ν(CO) modes [see (A)]; and free CO trapped by myoglobin (green). Each data set is scaled to unity at its maximum value. Figure from ref 35. Reprinted with permission from AAAS.

HydG radical reaction with an alternative substrate, 4-hydroxy phenyl propanoic acid (HPPA), where a simple C(2)H$_2$ replaces the C$_\alpha$H−NH$_2$ of tyrosine. An intense HPPA-derived radical EPR signal was observed, with major spin density on the C2 carbon as measured in a parallel reaction employing ^{13}C−C2 labeled HPPA. Thus, it was clear that the initial 5′dAdo$^\bullet$ H atom abstraction forms a transient, unobserved amino-nitrogen centered tyrosine radical that fragments into the RFQ-observed 4-oxidobenzyl radical and dehydroglycine (DHG), the intermediate source of the CO and CN$^-$ ligands to Fe of the H-cluster. We have no direct experimental information bridging between the contemporaneous formation of the 4-oxidobenzyl radical and DHG and the CO and CN$^-$ vibrational modes of these Fe-bound species as detected in HydG by stopped flow FTIR (Figure 6),[35] but we have recently developed a model for the intervening reactions using quantum chemistry methods to evaluate the energetics of possible reaction intermediates.[45]

Dehydroglycine is unstable in water and typically hydrolyzes to ammonia and glyoxylate.[31] In this case, the DHG is created by the tyrosine fission at the rSAM end of the TIM-barrel, with the "dangler Fe" of the five-Fe auxiliary cluster (vide infra) found at the other end. In essence, the space inside this barrel is a functions as a nanoreactor that guides the DHG conversion to a different product: organometallic Fe−CO and Fe−CN. (See also refs 46 and 47.) The initial reactants in our computational study are the 4-oxidobenzyl radical and DHG, and our proposed model, supported by the calculation of low energy barriers, is that the initial reactions involve a radical relay, with the 4-OB$^\bullet$ radical abstracting a H atom from the imine group nitrogen of DHG to form a DHG$^\bullet$ radical (ΔG = −4 kcal/mol; $\Delta G^\ddagger$ = 18 kcal/mol). The newly formed DHG$^\bullet$ radical then undergoes a homolytic C−C bond cleavage (ΔG = +4 kcal/mol; $\Delta G^\ddagger$ = 15 kcal/mol) to form a COO$^{\bullet-}$ radical

and HCN: thus, the conjugate acid of CN$^-$ is formed without direct involvement of the dangler Fe. It is interesting that in this model the 4-OB$^\bullet$ is not simply quenched to form *p*-cresol but plays a direct role in fragmenting the concomitantly formed DHG along the reactions pathway to Fe-bound CO and CN$^-$ in preference to ammonia and glyoxylate. In the next step, the COO$^{\bullet-}$ radical forms CO at the dangler Fe site, so we need to describe that site in some detail before returning.

Module 2: Formation of the Catalytically Relevant Resting State of HydG, the Cysteine-Chelated Dangler Fe(II) Complex at the Auxiliary Cluster

Evidence: X-ray Crystal Structures, Protein Mutagenesis, EPR Spectroscopy, and Mössbauer Spectroscopy (See Figure 5 M2). In addition to resolving the [4Fe−4S] radical SAM cluster of *Ti*HydG, the Dinis et al. structure[41] revealed that the auxiliary cluster is not a routine [4Fe−4S] cluster but includes a unique fifth Fe site coupled to the site differentiated Fe (the one without ligation by a cysteine residue) of a [4Fe−4S] cluster, with the ligation assigned to a sulfide bridge. The *Ti* structure assigns another fifth Fe ligand to a conserved histidine(265) *trans* to the sulfide, chelated by an unassigned amino acid, with two water ligands completing the coordination sphere. This structure also provided a likely site for the origin of Fe−CO and Fe−CN FTIR signals (vide infra), as the fifth Fe is located at the other end of the 24 Å barrel from the rSAM cluster and therefore positioned to bind CO and CN$^-$ created by the rSAM tyrosine lysis, presumably initially at the two water sites. However, the reported occupancy of the fifth Fe site is relatively low, with 0.73 in one monomer of the structure and zero in the other. In addition, the presence of a high spin S = 2 Fe(II) linked to a S = 1/2 [4Fe−4S]$^{+1}$ cluster opened a window to the assignment of the previously reported high spin (S = 5/2) FeS EPR signal with effective *g*-values of 9.5, 4.7, 4.1, and 3.8,[43] consistent with its being observed under reducing conditions[41] (under oxidizing conditions, high spin Fe(III) can give rise to various high spin EPR signals, even when bound adventitiously to proteins).

This X-ray crystal structure was followed by Suess's "cysteine hypothesis".[38] The Dinis et al.[41] *Ti*HydG structure does not fully define the ligation of the dangler Fe. Suess et al.[38] further probed the nature of the high spin EPR signal previously assigned to the reduced S = 1/2 [4Fe−4S]$^{+1}$ auxiliary cluster coupled to the S = 2 dangler Fe. Treatment of *S. oneidensis* *So*HydG with ethylenediaminetetraacetic acid (EDTA) removes the fifth "dangler Fe" and converts the high spin EPR signal to a new, distinct S = 1/2 signal. Treatment with excess Fe(II) cleanly regenerates the high spin signal; thus, the dangler Fe can be reversibly removed and reintroduced with its presence or absence modulating the spin state of the auxiliary cluster. Moreover, if instead of reintroducing S = 2 Fe(II), the S = 1 Ni(II) ion is introduced following the EDTA depletion step, a new S = 3/2 signal appears, resulting from the [4Fe−4S]$^{+1}$ auxiliary cluster coupling to a spin S = 1 ion (Ni) rather than the original S = 2 ion (Fe) ion which gives rise to the initial S = 5/2 coupled signal. This work sets the stage for ^{57}Fe Mössbauer experiments, which involved fully labeled *So*HydG, a mutant with the rSAM cluster deleted, and specific EDTA Fe removal with ^{57}Fe reinstalled, all indicating the high spin Fe EPR signal arises from the 5Fe form of the auxiliary cluster and confirming that the dangler Fe(II) itself is high spin S = 2. Inspired in part by the need for cysteine in the cocktail of small

molecules needed for in vitro H-cluster maturation,[26] Suess et al.[38] tested the idea that cysteine can replace the bridging sulfide plus unidentified amino acid in the *Ti*HydG structure. This work showed that several "dangler deficient" samples were converted to the $S = 5/2$ form by the addition of exogenous cysteine, leading to a model that cysteine ligates the dangler Fe in a tridentate mode with its carboxylate, amino, and thiolate donors, with the HydG histidine residue providing the sole HydG protein ligand. In addition, to show that these experiments are not just the result of some physiochemical formation of a "junk Fe" type signal,[48] experiments were repeated with L-cysteine replaced with D-cysteine, L-homo-cysteine, L-alanine plus S^{2-}, or L-serine, none of which restore the $S = 5/2$ EPR signal now assigned to the dangler/L-cysteine complex bound at a specific site in the enzyme. Since following EDTA washing, the $S = 5/2$ signal is converted to a clean $S = 1/2$ form, Suess et al.[38] tested whether cysteine is still bound to the [4Fe−4S] cluster of the auxiliary cluster by using electron nuclear double resonance (ENDOR) with a 3-^{13}C-labeled cysteine added, with a well simulated ^{13}C ENDOR doublet resulting. Thus, in this model, the resting state converts from a [4Fe−4S]cysteine $S = 1/2$ cluster to the active five-Fe $S = 5/2$ form with the addition of the high spin dangler Fe(II), providing the assembly site for building an organometallic Fe center as needed for H-cluster formation.[38]

We also note that homocysteine was also modeled as a chelating Fe ligand[47] in a similar reinterpretation of the Dinis et al.[41] structure, though, unlike cysteine, we found that homocysteine did not stabilize the $S = 5/2$ EPR signal or enable the HydG FTIR signals in dangler-deficient HydG preparations.[38,49]

Module 3: Formation of Complex A, the First Organometallic Intermediate: An Fe(II)(CO)(CN)cysteine Complex

Evidence: FTIR and EPR Spectroscopy and Quantum Chemistry (See Figure 5 M3). The initial evidence for a Fe(II)(CO)(CN) organometallic intermediate within the HydG enzyme was in a time-resolved stopped flow FTIR study undertaken to detect any CO and/or CN vibrational features whose frequencies and intensities would be sensitive to coordination to Fe.[35] The use of tyrosine isotopologues allowed for straightforward ^{13}C and ^{15}N labeling and measurements of the resulting isotope shifts with increased reduced mass. Figure 6A shows FTIR spectra at selected times following the reaction initiation by mixing *So*HydG, [13]C$_9$-Tyr, SAM, and sodium dithionite (DTH).[35] At around 30 s, we observe new isotope sensitive Fe−CO and Fe−CN modes (see table in Figure 1D in ref 35) assigned to an intermediate called "Complex A". Figure 6B shows the time dependence of the observed FTIR signals overlaid with intensity vs RFQ time for the 4OB[•] radical EPR signal.[43] It is noteworthy that the Complex A Fe(II)(CO)(CN) signal rises on the same time scale as the decay of the 4OB[•] signal, which indicates that, in the strep-tag isolated *So*HydG preparations, the tyrosine-derived DHG is rapidly converted to Fe-bound CO and CN− without a notable time delay. Complex A has also been well characterized with freeze-quenched continuous wave (CW) and pulse electron paramagnetic resonance (EPR) spectroscopy.[50] With the addition of the two strong field diatomic ligands, the high spin Fe(II) of the resting state converts to low spin, which effectively decouples the dangler Fe magnetically from the [4Fe−4S][+1] cluster, converting the spin state of the

five-iron auxiliary cluster from $S = 5/2$ to $S = 1/2$. Pulse EPR reveals weak couplings to magnetic nuclei introduced into the dangler moiety, specifically to [57]Fe, [13]CN, [13]CO, and 3-^{13}C-cysteine, with the small magnitude of the couplings rationalized in that the residual paramagnetism is now only localized on the [4Fe−4S][+1] because the prior Fe(II) magnetism is now quenched by the CO and CN− ligation.

We have explored the formation of Complex A with the QM/MM approach, picking up where we left off in Module 1.[45] At this point in the sequential model (end of Module 1), the radical cascade has already produced the CN−, initially in the form of the weakly acidic ($pK_a = 9.2$) HCN, and this can replace one of waters bound to the dangler Fe in the resting state. The radical cascade also produces the COO[•−] radical. It is plausible to assume that COOH[•] is protonated because there is a Glu residue adjacent this radical and the computed energy difference between Glu + COOH[•] and GluH + COO[•−] is about 5 kcal/mol, indicating that these two states may be interchangeable. Because the reduction of COO[•−] is coupled to proton transfer, the assumption of protonated COOH[•] allows for the discussion to focus on reduction. COOH[•] binds at the other resting state water position where it is converted to the CO ligand of Complex A via a proton-coupled electron transfer, with an overall $\Delta G = -21.1$ kcal/mol and a $\Delta G^{\ddagger}$ of 12.9 kcal/mol. This pathway provides a thermodynamically accessible pathway to the first organometallic intermediate on the path to the H-cluster, the kinetically defined Complex A intermediate of HydG.

A similar CO/CN− formation mechanism on the dangler Fe site was also hypothesized by Pagnier et al.,[47] although in our calculations this polar mechanism has a higher energy barrier for the decomposition of DHG into CN− and CO relative to the radical relay described above.

Module 4: Formation of Complex B and Release of the HydG Product, a [Fe(II)(CN)(CO)$_2$(cysteinate)]− Synthon

Evidence: FTIR and EPR Spectroscopy and Quantum Chemistry (See Figure 5 M4). The next signal arising in the stopped flow FTIR spectra of HydG is a Fe(CO)$_2$CN intermediate designated "Complex B" (Figure 6A).[35] Forming this intermediate necessitates a second round of tyrosine lysis at the rSAM cluster, and it is notable that only the second CO appears to bind to the unique Fe, without a second coupled CN− evidenced in the FTIR spectra. The time scale for Complex B formation is appreciably slower, by a factor of 10 compared to Complex A formation (Figure 6B). This is perhaps not surprising as Complex A formation begins with the high spin dangler Fe(II) with two water ligands, the active resting state of the enzyme, whereas Complex B formation starts with Complex A already formed, with a low spin Fe(II) with the first CO and CN− ligands already in place. The RFQ CW and pulse EPR on this time scale shows a new signal assigned to a [4Fe−4S]CN species..[38,51] Suess et al.[38] proposed that this cyanide binding to the [4Fe−4S][+1] cluster is the trigger for releasing the actual HydG product, a [Fe(II)(CN)(CO)$_2$(cysteinate)]− species often referred to as "the synthon". Of course, since only one CN− ligand is needed per Fe in the [2Fe]$_H$ subcluster, a second CN− ligand is not needed in the synthon, and it is intriguing that the second CN− plays this specific role, to release the HydG product synthon, previously tightly bound, at the exact point where it can be transferred to the other maturases for the next steps in assembly.

In the sequential model, the initial radical SAM chemistry is repeated in building Complex B through the formation of CN^- and the $COOH^\bullet$ radical (Module 1, repeated). The unique new aspect is how the $COOH^\bullet$ radical reacts with the already formed organometallic species, Complex A. An energetically accessible route is for the $COOH^\bullet$ radical to form a C−C bond with the Fe-bound CO to form a new intermediate with a oxalyl (OC−COOH) ligand to Fe, with calculated $\Delta G = -4.0$ kcal/mol and $\Delta G^{\ddagger} = 6.4$ kcal/mol. In the next step, a similar proton/electron transfer results in the decomposition of the glyoxylyl ligand to form the second CO and a water. This step has the highest computed barrier in our HydG model: $\Delta G = -12.6$ kcal/mol and $\Delta G^{\ddagger} = 21.8$ kcal/mol, perhaps explaining why the Complex B formation kinetics are relatively slow. The second CO is then able to displace the 5-MIm ligand with $\Delta G = -12.5$ and $\Delta G^{\ddagger} = 14.6$ kcal/mol. The displacement of the synthon by the second CN^- is calculated to be barrier free, with $\Delta G = 0.85$ kcal/mol. The replacement of CN^- by CH_3SH, the side chain analogue of cysteine, closes the catalytic cycle with $\Delta G = 1.0$ and $\Delta G^{\ddagger} = 16.0$ kcal/mol.

An Important Reality Check: Can a Synthetic $[Fe(II)(CN)(CO)_2(cysteinate)]^-$ Donor Replace HydG in H-Cluster Synthesis? The Answer Is Yes

Evidence: EXAFS Spectroscopy. As noted, synthetic precursors have been used successfully in the artificial maturation of apo-HydA, employing a dinuclear Fe synthetic precursor $[(Fe_2(adt)(CN)_2(CO)_4]^{2-}$ to the $[2Fe]_H$ subcluster.[27,28] In turn, the proposed $[Fe(CN)(CO)_2(cysteinate)]^-$ product of the dual enzymatic action of HydG provided an intriguing synthetic target for the Rauchfuss laboratory at the University of Illinois, who developed a convenient synthetic carrier of this proposed synthon termed "Syn-B".[39,52] In the maturation of the [FeFe] hydrogenase H-cluster, HydG and tyrosine are absolutely required for hydrogenase activity.[26] However, the maturation with Syn-B in place of HydG/ tyrosine, all other conditions identical, provides activity comparable to that of the conventional maturation using all three maturases; thus, a synthetic version of the proposed HydG synthon product enables effective H-cluster semisynthesis to be pushed back now to the level of a mononuclear Fe organometallic species, strongly supporting the sequential synthetic model for its biosynthesis. Moreover, the $[Fe(II)-(CN)(CO)_2(cysteinate)]^-$ component of Syn-B can be easily made with isotope labels or chemical substitutions which can be used to track the origin of components of the assembled H-cluster. Specifically, we now know, based on EXAFS (both Se and Fe edge) comparing the H-cluster synthesized with selenocysteine-Syn-B vs cysteine-Syn-B, that the anchoring sulfur components of the adt bridge are sourced from the synthon's cysteine sulfur.[39] Given that this synthetic version of the proposed HydG product can replace the otherwise essential HydG, it can in turn be used to test how this synthon acts in concert with the remaining maturases HydE and HydF. Specifically, we find that the $[Fe(II)(CN)-(CO)_2(cysteinate)]^-$ is bound by the second radical SAM enzyme HydE adjacent to its [4Fe−4S]-SAM active site and that the function of HydE is to activatate the $[Fe(II)(CN)-(CO)_2(cysteinate)]^-$ for dimerization, initially by forming an adenosylated Fe(I) complex as described in the following section.

HydE

Evidence: EPR spectroscopy

Compared to HydG, a thorough description of the mechanism of the radical SAM enzyme HydE came slowly because its actual substrate was unknown. Given its role in bypassing HydG/tyrosine in the semisynthesis of the H-cluster, we tested whether the $[Fe(CN)(CO)_2(cysteinate)]^-$ species could be the substrate for HydE, again by using the synthon donor complex Syn-B. Tao et al.[53] showed with EPR spectroscopy that the radical SAM reaction of HydE indeed catalyzes the conversion of the HydG produced synthon, initially forming the adenosylated Fe(I) intermediate via a the 5′dAdo$^\bullet$ attack on the cysteine sulfur of the synthon. This spectroscopic study was soon followed by an X-ray crystallography study by Rohac et al.[54] showing the specific binding site of the synthon adjacent to the rSAM [4Fe−4S] cluster.

Module 5: The $[Fe(II)(CN)(CO)_2(cysteinate)]^-$ Binds as the Substrate in HydE

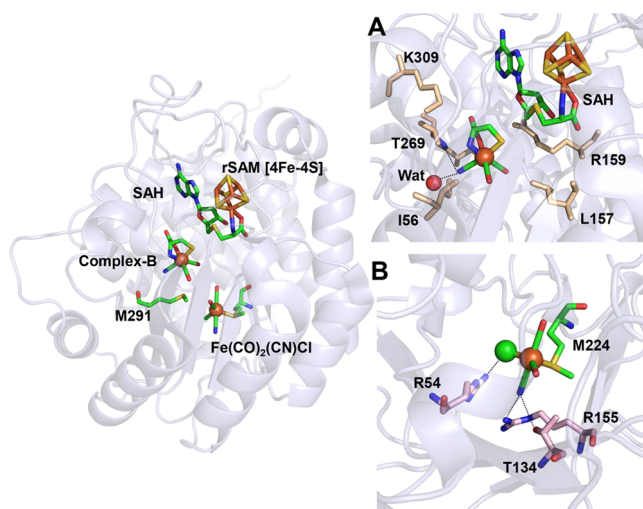**Evidence: X-ray Crystallography and EPR Spectroscopy.** Figure 7 summarizes recent *Thermotoga maritima*

Figure 7. Summary of crystal structures of *Thermotoga maritima* *Tm*HydE interacting with Syn-B-donated $[Fe(CN)-(CO)_2(cysteinate)]^-$, from PDB entry 7O1T.[54]

*Tm*HydE crystal structures obtained by crystallizing this rSAM enzyme with the synthon carrier Syn-B.[54] Figure 7A zooms in on the substrate binding site as found in the "upper part" of HydE's β barrel cavity. For this component of the HydE crystal stucture study, focusing on the substrate binding site, the nonreactive SAM analogue (S)-adenosyl-L-homocysteine (SAH) was used in place of SAM. The position of the CN^- ligand relative to the two CO ligands to the central Fe cannot be directly determined given the small differences in electron densities but is instead assigned based on the protein surroundings, with the CN^- ligand *trans* to the cysteine sulfur in a position that enables hydrogen bonding, while the two CO ligands occupy hydrophobic pockets, following the reasoning of such assignments of the original [FeFe] hydrogenase structures.[55−57] Importantly, the bound synthon is oriented with the cysteine sulfur adjacent to the [4Fe−4S]−SAH complex, consistent with the EPR determined 5′dAdo$^\bullet$ cross-linking with the sulfur in the first kinetically resolved reaction intermediate on the 10 s time scale..[53] This is also analogous to
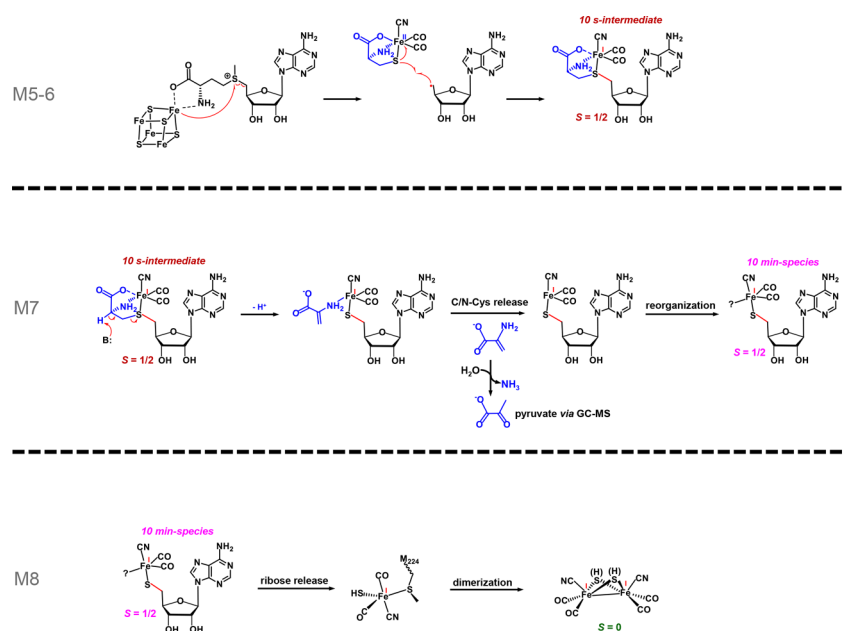
Figure 8. Detailed reaction modules (M5−M8) of the radical SAM enzyme HydE.

prior structures of HydE reacting with nonphysiological thiazolidine compounds and showing similar adenosyl-cysteine cross-links.[58]

Module 6: The Radical SAM Chemistry of HydE Produces an Adenosylated [Fe(I)(CO)$_2$(CN)cysteine] Complex

Evidence: EPR, Mass Spectrometry, and X-ray Crystallography. After about 10 s following rSAM reaction initiation, freeze quenched EPR samples show the presence of a $S = 1/2$ adenosylated $[\text{Fe(I)(CO)}_2\text{(CN)cysteine}]$ species generated from HydE's radical reaction with the Syn-B donated $[\text{Fe(CN)(CO)}_2\text{(cysteinate)}]^-$ (Figure 8 M5-6).[53] Instead of doing the canonical H atom abstraction, here the 5′dAdo[•] radical attacks the cysteine sulfur to form a C5′-S bond[58] along with the reduction of Fe(II) to Fe(I). This assignment is based on the CW EPR measured g-tensor as well as pulse EPR measurements employing Syn-B and SAM nuclear spin isotopologues. Mass spectrometry also detected (S)-adenosyl-L-cysteine with the appropriate isotope shifts, along with the predicted mass change when using selenocysteine-Syn-B. In addition, Rohac et al.[54] crystallized TmHydE subsequent to initiating the radical SAM reactions with Syn-B, or selenocysteine-Syn-B, and they observe (S)-adenosyl-L-cysteine, or alternatively (S)-adenosyl-L-selenocysteine, bound to the [4Fe−4S] cluster (not shown).

Module 7: HydE Cleavage of the Cysteine C−S Bond Leads to a Five-Coordinate [Fe(I)S(CO)$_2$CN] Complex

Evidence: EPR and Mass Spectrometry. The detected 10 s intermediate converts to a new $S = 1/2$ Fe(I) complex over time (approx 10 min) within HydE (Figure 8 M7).[53] The internal cysteine 3C−S bond is cleaved, generating pyruvate as previously observed by mass spectrometry in the full maturation,[39] but now localizing this reaction specifically to HydE.[53] Pulse EPR shows that this new intermediate retains the two CO and one CN$^-$ ligand along with the adenosyl linkage. The presence of a possible ribose O4′ ligand at this stage as previously modeled[53] is unclear.

Module 8: Ribose Release and Dimerization

Evidence: EPR Signal Quenching and X-ray Crystallography. As noted, Rohac et al. also crystallized TmHydE following the reaction with Syn-B, or selenocysteine-Syn-B, and they observed what is modeled as a FeCl(CO)$_2$CN complex associated with methionine-224 in a lower portion of the TIM barrel Figure 7. As Cl is isostructural with SH, we suggest this may result as a degradation of a transient FeS(CO)$_2$CN species that is on a path to dimerization, resulting in an antiferromagnetically coupled $S = 0$ $[(\text{Fe-(I)})_2\text{S}_2\text{(CO)}_4\text{(CN)}_2]$ dimer, consistent with the loss of the 10 min $S = 1/2$ intermediate EPR signal (Figure 8 M8). Thus, in this kinetic model, the initial dimer formation leading to the $[2\text{Fe}]_H$ cluster occurs on HydE, leaving some combination of HydF, HydA, and enzymes in the *E. coli* lysate to install the CH$_2$NHCH$_2$ component of the adt bridge for the completion of the $[2\text{Fe}]_H$ subcluster.

■ CONCLUSIONS, REMAINING CONTROVERSIES, AND OPEN QUESTIONS

In this Perspective, we have presented a detailed overview of the roles we have assigned to the radical SAM enzymes HydG and HydE in assembling an organometallic $[\text{Fe}_2\text{S}_2\text{(CO)}_4\text{(CN)}_2]$ dinuclear Fe(I) precursor to the $[2\text{Fe}]_H$ subcluster of [FeFe] hydrogenase. We also noted a prior model for the role of the maturases in H-cluster assembly, in which the adt bridge and CO and CN$^-$ are proposed to be produced by the HydG and HydE, which then redecorate a pre-existing 2Fe−2S cluster on HydF.[23,32−34] There is a certain elemental simplicity to this earlier model, but it raises a number of important questions. For example, how are four anchoring cysteine ligands from this [2Fe−2S] cluster on HydF removed and replaced with free CO, CN$^-$, and a preassembled azadithiolate moiety, all with the proper stoichiometry and stereochemistry, while keeping the preexisting cluster intact? What is the fate of these four cysteines? And how does the cell handle the delivery of cytotoxic CO and CN$^-$ ligands? The sequential assembly model is supported by much experimental data as noted in the prior sections. It invokes a cysteine

cosubstrate to bind the dangler Fe and thereby avoids anchoring a kinetically inert, low-spin octahedral Fe(II) center to the protein. This complex is transferred to HydE, where its kinetic inertness is overcome by the unusual radical chemistry of HydE: the cysteine ligand is removed by the formation of a weak thioether ligand and by the generation of Fe(I), which is unstable in an octahedral configuration.

One open question that deserves further comment is the production of free CO in turnover experiments with the isolated rSAM enzyme HydG.[35] In the sequential model, the role of HydG is to lyse two tyrosines and build a $[Fe(II)(CN)(CO)_2(cysteinate)]^-$ that is transferred to HydE where it acts as the substrate for this second radical SAM enzyme. It is not surprising that the product of HydG, if not properly transferred and activated for dimerization, might instead result in some free CO or that free CO might be produced from the DHG product of the tyrosine lysis in some quantity, depending on the conditions of the enzyme such as the intactness of the Fe(II)cysteine complex linked to the auxiliary [4Fe−4S] cluster or illumination during an optical spectroscopy assay that could drive incidental Fe−CO photolysis.[59] For example, FTIR spectroscopy clearly shows that proper installation of the dangler Fe/cysteine resting state of SoHydG (as assayed by EPR spectroscopy) is required for high yields of the Complex A and Complex B intermediates.[49] It is noteworthy that using UV/vis spectroscopy of CO binding to exogenous heme as a sole technique does not allow the detection of the HydG Fe−CO/CN⁻ species reported as Complex A and Complex B in SoHydG HydG.[35,49] In our FTIR study with 1 mM myoglobin added to the SoHydG ([HydG] = 6.25 μM)) reaction, we detect CO bound to myoglobin (1944 cm⁻¹) after about a 2 min lag phase and thereafter rising with a rate of about 0.038 min⁻¹ (from linear replotting of data previously reported,[35] Simon J. George, personal communication). In the most recent paper supporting the relevance of free CO in the H-cluster assembly,[48] the authors examine C. acetobutylicum (Ca) HydG and present their newest results for optimized CO detection using absorbance changes at 425 nm of a H64L variant of Physeter macrocephalus myoglobin. They report "burst phase" rates (linear fit between 0 and 5 min) on the order of 0.09 min⁻¹, somewhat higher than what we observed in this prior FTIR study. However, the major point to be made is this is far slower than the formation of the internal HydG Fe−CO/CN⁻ species observed via FTIR (and not measured in their optical detection with myoglobin experiments). As noted, in SoHydG, the first organometallic intermediate, Complex A, rises synchronously with the decay of the 4OB• radical and with a rate of 14 min⁻¹ or about 150 times faster than the free CO detected in the optimized assay by Shepard et al.[48] in CaHydG. The conversion to the HydG $[Fe(II)(CN)(CO)_2(cysteinate)^-$ product, recorded as FTIR signal Complex B, is slower as described earlier in this Perspective but with a rate of 0.54 min⁻¹, appreciably faster than the rates reported for free CO production. So although we agree that HydG can produce free CO, with details dependent on the specific form of HydG along with various preparation conditions, this is slow compared to the internal formation of Fe−CO/CN⁻ organometallic intermediates in SoHydG, and we therefore do not consider it catalytically relevant. An important caveat to this conclusion is that although we have used time-resolved FTIR to compare CO release to Complex A and Complex B formation kinetics in SoHydG as described, no FTIR data have

been reported for CaHydG in this recent report of free CO release,[48] and such an internally consistent comparison between free CO production and any observed organometallic intermediates produced within CaHydG would be highly useful for helping to resolve this controversy.

There are remaining issues to be resolved in the sequential biosynthesis model. Continuing in the FTIR arena, with a new quantum chemistry model for the detailed formation of Complex B via a transient glyoxylyl ligand to Fe (M4), it would be useful to perform new FTIR experiments designed to test this model. We suggest (M8) that the initial formation of a $[Fe(I)_2S_2(CO)_4(CN)_2]$ dimer occurs as a last step in the HydE mechanism, but that remains a conjecture at this point. What follows in conjecture is a possible catalytic role for HydF beyond its serving as a docking platform for the assembled $[2Fe]_H$ cluster before its transfer to HydA for H-cluster completion (Figure 3 M11). If the proposed $[Fe(I)_2S_2(CO)_4(CN)_2]$ HydE product binds at HydF, then it is left to HydF to be the site of completion of the azadithiolate bridge, adding the CH_2NHCH_2 component as derived from the 3-C and amino-N of serine,[40] possibly with yet defined contributions by components of the E. coli lysate present in our current in vitro maturation protocol (Figure 3 M9, 10).

Another topic for future exploration is defining the specific protein−protein interactions that enable the biosynthetic cycle and gaining a detailed knowledge of how unstable intermediates are passed from one maturase to the next. For example, in the sequential model, how is the HydG synthon product passed to HydE and loaded into the defined substrate site adjacent to HydE's [4Fe−4S]SAM cluster? Following that, how is the HydE product transferred to HydF? No doubt there will soon be progress in further defining these crucial protein−protein interactions.

■ AUTHOR INFORMATION

Corresponding Author

R. David Britt − Department of Chemistry, University of California, Davis, Davis, California 95616, United States; orcid.org/0000-0003-0889-8436; Email: rdbritt@ucdavis.edu

Authors

Lizhi Tao − Department of Chemistry, University of California, Davis, Davis, California 95616, United States; orcid.org/0000-0001-9921-2297

Guodong Rao − Department of Chemistry, University of California, Davis, Davis, California 95616, United States; orcid.org/0000-0001-8043-3436

Nanhao Chen − Department of Chemistry, University of California, Davis, Davis, California 95616, United States

Lee-Ping Wang − Department of Chemistry, University of California, Davis, Davis, California 95616, United States; orcid.org/0000-0003-3072-9946

Complete contact information is available at:
https://pubs.acs.org/10.1021/acsbiomedchemau.1c00035

Notes

The authors declare no competing financial interest.

maturation and Simon J. George for discussions on free CO production as measured by FTIR.[35]

■ ABBREVIATIONS

CW EPR, continuous wave electron paramagnetic resonance; ENDOR, electron nuclear double resonance; EXAFS, X-ray absorption fine structure spectroscopy; FTIR, Fourier transform infrared; HYSCORE, hyperfine sublevel correlation spectroscopy

■ REFERENCES

(1) Peters, J. W.; Broderick, J. B. Emerging Paradigms for Complex Iron-Sulfur Cofactor Assembly and Insertion. *Annu. Rev. Biochem.* **2012**, *81*, 429−450.

(2) Ribbe, M. W.; Hu, Y. L.; Hodgson, K. O.; Hedman, B. Biosynthesis of Nitrogenase Metalloclusters. *Chem. Rev.* **2014**, *114*, 4063−4080.

(3) Britt, R. D.; Rao, G. D.; Tao, L. Z. Bioassembly of complex iron-sulfur enzymes: hydrogenases and nitrogenases. *Nature Reviews Chemistry* **2020**, *4*, 542−549.

(4) Madden, C.; Vaughn, M. D.; Diez-Perez, I.; Brown, K. A.; King, P. W.; Gust, D.; Moore, A. L.; Moore, T. A. Catalytic Turnover of FeFe -Hydrogenase Based on Single-Molecule Imaging. *J. Am. Chem. Soc.* **2012**, *134*, 1577−1582.

(5) Pandey, K.; Islam, S. T. A.; Happe, T.; Armstrong, F. A. Frequency and potential dependence of reversible electrocatalytic hydrogen interconversion by FeFe -hydrogenases. *Proc. Natl. Acad. Sci. U. S. A.* **2017**, *114*, 3843−3848.

(6) Kanygin, A.; Milrad, Y.; Thummala, C.; Reifschneider, K.; Baker, P.; Marco, P.; Yacoby, I.; Redding, K. E. Rewiring photosynthesis: a photosystem I-hydrogenase chimera that makes H2 in vivo. *Energy Environ. Sci.* **2020**, *13*, 2903−2914.

(7) Appel, J.; Hueren, V.; Boehm, M.; Gutekunst, K. Cyanobacterial in vivo solar hydrogen production using a photosystem I-hydrogenase (PsaD-HoxYH) fusion complex. *Nature Energy* **2020**, *5*, 458−467.

(8) Kleinhaus, J. T.; Wittkamp, F.; Yadav, S.; Siegmund, D.; Apfel, U.-P. [FeFe]-Hydrogenases: maturation and reactivity of enzymatic systems and overview of biomimetic models. *Chem. Soc. Rev.* **2021**, *50*, 1668−1784.

(9) Mulder, D. W.; Guo, Y. S.; Ratzloff, M. W.; King, P. W. Identification of a Catalytic Iron-Hydride at the H-Cluster of FeFe -Hydrogenase. *J. Am. Chem. Soc.* **2017**, *139*, 83−86.

(10) Pelmenschikov, V.; Birrell, J. A.; Pham, C. C.; Mishra, N.; Wang, H. X.; Sommer, C.; Reijerse, E.; Richers, C. P.; Tamasaku, K.; Yoda, Y.; Rauchfuss, T. B.; Lubitz, W.; Cramer, S. P. Reaction Coordinate Leading to H-2 Production in FeFe -Hydrogenase Identified by Nuclear Resonance Vibrational Spectroscopy and Density Functional Theory. *J. Am. Chem. Soc.* **2017**, *139*, 16894−16902.

(11) Reijerse, E. J.; Pham, C. C.; Pelmenschikov, V.; Gilbert-Wilson, R.; Adamska-Venkatesh, A.; Siebel, J. F.; Gee, L. B.; Yoda, Y.; Tamasaku, K.; Lubitz, W.; Rauchfuss, T. B.; Cramer, S. P. Direct Observation of an Iron-Bound Terminal Hydride in FeFe -Hydrogenase by Nuclear Resonance Vibrational Spectroscopy. *J. Am. Chem. Soc.* **2017**, *139*, 4306−4309.

(12) Land, H.; Senger, M.; Berggren, G.; Stripp, S. T. Current State of [FeFe]-Hydrogenase Research: Biodiversity and Spectroscopic Investigations. *ACS Catal.* **2020**, *10*, 7069−7086.

(13) Angamuthu, R.; Chen, C. S.; Cochrane, T. R.; Gray, D. L.; Schilter, D.; Ulloa, O. A.; Rauchfuss, T. B. N-Substituted Derivatives of the Azadithiolate Cofactor from the FeFe Hydrogenases: Stability and Connplexation. *Inorg. Chem.* **2015**, *54*, 5717−5724.

(14) Britt, R. D.; Rao, G. D.; Tao, L. Z. Biosynthesis of the catalytic H-cluster of FeFe hydrogenase: the roles of the Fe-S maturase proteins HydE, HydF, and HydG. *Chemical Science* **2020**, *11*, 10313−10323.

(15) Posewitz, M. C.; King, P. W.; Smolinski, S. L.; Zhang, L. P.; Seibert, M.; Ghirardi, M. L. Discovery of two novel radical S-adenosylmethionine proteins required for the assembly of an active Fe hydrogenase. *J. Biol. Chem.* **2004**, *279*, 25711−25720.

(16) Rubach, J. K.; Brazzolotto, X.; Gaillard, J.; Fontecave, M. Biochemical characterization of the HydE and HydG iron-only hydrogenase maturation enzymes from Thermatoga maritima. *FEBS Lett.* **2005**, *579*, 5055−5060.

(17) King, P. W.; Posewitz, M. C.; Ghirardi, M. L.; Seibert, M. Functional studies of FeFe hydrogenase maturation in an Escherichia coli biosynthetic system. *J. Bacteriol.* **2006**, *188*, 2163−2172.

(18) McGlynn, S. E.; Ruebush, S. S.; Naumov, A.; Nagy, L. E.; Dubini, A.; King, P. W.; Broderick, J. B.; Posewitz, M. C.; Peters, J. W. In vitro activation of FeFe hydrogenase: new insights into hydrogenase maturation. *JBIC, J. Biol. Inorg. Chem.* **2007**, *12*, 443−447.

(19) Mulder, D. W.; Ortillo, D. O.; Gardenghi, D. J.; Naumov, A. V.; Ruebush, S. S.; Szilagyi, R. K.; Huynh, B.; Broderick, J. B.; Peters, J. W. Activation of HydA(Delta EFG) Requires a Preformed 4Fe-4S Cluster. *Biochemistry* **2009**, *48*, 6240−6248.

(20) Mulder, D. W.; Boyd, E. S.; Sarma, R.; Lange, R. K.; Endrizzi, J. A.; Broderick, J. B.; Peters, J. W. Stepwise FeFe -hydrogenase H-cluster assembly revealed in the structure of HydA(Delta EFG). *Nature* **2010**, *465*, 248−U143.

(21) Pilet, E.; Nicolet, Y.; Mathevon, C.; Douki, T.; Fontecilla-Camps, J. C.; Fontecave, M. The role of the maturase HydG in FeFe -hydrogenase active site synthesis and assembly. *FEBS Lett.* **2009**, *583*, 506−511.

(22) Driesener, R. C.; Challand, M. R.; McGlynn, S. E.; Shepard, E. M.; Boyd, E. S.; Broderick, J. B.; Peters, J. W.; Roach, P. L. FeFe -Hydrogenase Cyanide Ligands Derived From S-Adenosylmethionine-Dependent Cleavage of Tyrosine. *Angew. Chem., Int. Ed.* **2010**, *49*, 1687−1690.

(23) Shepard, E. M.; Duffus, B. R.; George, S. J.; McGlynn, S. E.; Challand, M. R.; Swanson, K. D.; Roach, P. L.; Cramer, S. P.; Peters, J. W.; Broderick, J. B. FeFe -Hydrogenase Maturation: HydG-Catalyzed Synthesis of Carbon Monoxide. *J. Am. Chem. Soc.* **2010**, *132*, 9247−9249.

(24) Vallese, F.; Berto, P.; Ruzzene, M.; Cendron, L.; Sarno, S.; De Rosa, E.; Giacometti, G. M.; Costantini, P. Biochemical Analysis of the Interactions between the Proteins Involved in the FeFe -Hydrogenase Maturation Process. *J. Biol. Chem.* **2012**, *287*, 36544−36555.

(25) Lubitz, W.; Ogata, H.; Rudiger, O.; Reijerse, E. *Chem. Rev.* **2014**, *114*, 4081−4148.

(26) Kuchenreuther, J. M.; Britt, R. D.; Swartz, J. R. New Insights into FeFe Hydrogenase Activation and Maturase Function. *PLoS One* **2012**, *7*, e45850.

(27) Berggren, G.; Adamska, A.; Lambertz, C.; Simmons, T. R.; Esselborn, J.; Atta, M.; Gambarelli, S.; Mouesca, J. M.; Reijerse, E.; Lubitz, W.; Happe, T.; Artero, V.; Fontecave, M. Biomimetic assembly and activation of FeFe -hydrogenases. *Nature* **2013**, *499*, 66−70.

(28) Esselborn, J.; Lambertz, C.; Adamska-Venkatesh, A.; Simmons, T.; Berggren, G.; Nothl, J.; Siebel, J.; Hemschemeier, A.; Artero, V.; Reijerse, E.; Fontecave, M.; Lubitz, W.; Happe, T. Spontaneous activation of FeFe -hydrogenases by an inorganic 2Fe active site mimic. *Nat. Chem. Biol.* **2013**, *9*, 607−609.

(29) Artero, V.; Berggren, G.; Atta, M.; Caserta, G.; Roy, S.; Pecqueur, L.; Fontecave, M. From Enzyme Maturation to Synthetic Chemistry: The Case of Hydrogenases. *Acc. Chem. Res.* **2015**, *48*, 2380−2387.

(30) Sommer, C.; Richers, C. P.; Lubitz, W.; Rauchfuss, T. B.; Reijerse, E. J. A RuRu Analogue of an FeFe -Hydrogenase Traps the Key Hydride Intermediate of the Catalytic Cycle. *Angew. Chem., Int. Ed.* **2018**, *57*, 5429−5432.

(31) Kriek, M.; Martins, F.; Challand, M. R.; Croft, A.; Roach, P. L. Thiamine biosynthesis in Escherichia coli: Identification of the intermediate and by-product derived from tyrosine. *Angew. Chem., Int. Ed.* **2007**, *46*, 9223−9226.

(32) Shepard, E. M.; Mus, F.; Betz, J. N.; Byer, A. S.; Duffus, B. R.; Peters, J. W.; Broderick, J. B. FeFe -Hydrogenase Maturation. *Biochemistry* **2014**, *53*, 4090−4104.

(33) Shepard, E. M.; McGlynn, S. E.; Bueling, A. L.; Grady-Smith, C. S.; George, S. J.; Winslow, M. A.; Cramer, S. P.; Peters, J. W.; Broderick, J. B. Synthesis of the 2Fe subcluster of the FeFe -hydrogenase H cluster on the HydF scaffold. *Proc. Natl. Acad. Sci. U. S. A.* **2010**, *107*, 10448−10453.

(34) Duffus, B. R.; Hamilton, T. L.; Shepard, E. M.; Boyd, E. S.; Peters, J. W.; Broderick, J. B. Radical AdoMet enzymes in complex metal cluster biosynthesis. *Biochim. Biophys. Acta, Proteins Proteomics* **2012**, *1824*, 1254−1263.

(35) Kuchenreuther, J. M.; Myers, W. K.; Suess, D. L. M.; Stich, T. A.; Pelmenschikov, V.; Shiigi, S. A.; Cramer, S. P.; Swartz, J. R.; Britt, R. D.; George, S. J. The HydG Enzyme Generates an Fe(CO)(2)(CN) Synthon in Assembly of the FeFe Hydrogenase H-Cluster. *Science* **2014**, *343*, 424−427.

(36) Myers, W. K.; Stich, T. A.; Suess, D. L. M.; Kuchenreuther, J. M.; Swartz, J. R.; Britt, R. D. The Cyanide Ligands of FeFe Hydrogenase: Pulse EPR Studies of C-13 and N-15-Labeled H-Cluster. *J. Am. Chem. Soc.* **2014**, *136*, 12237−12240.

(37) Rao, G. D.; Britt, R. D. Electronic Structure of Two Catalytic States of the FeFe Hydrogenase H-Cluster As Probed by Pulse Electron Paramagnetic Resonance Spectroscopy. *Inorg. Chem.* **2018**, *57*, 10935−10944.

(38) Suess, D. L. M.; Burstel, I.; De La Paz, L.; Kuchenreuther, J. M.; Pham, C. C.; Cramer, S. P.; Swartz, J. R.; Britt, R. D. Cysteine as a ligand platform in the biosynthesis of the FeFe hydrogenase H cluster. *Proc. Natl. Acad. Sci. U. S. A.* **2015**, *112*, 11455−60.

(39) Rao, G.; Pattenaude, S. A.; Alwan, K.; Blackburn, N. J.; Britt, R. D.; Rauchfuss, T. B. The binuclear cluster of [FeFe] hydrogenase is formed with sulfur donated by cysteine of an [Fe(Cys)(CO)2(CN)] organometallic precursor. *Proc. Natl. Acad. Sci. U. S. A.* **2019**, *116*, 20850−20855.

(40) Rao, G. D.; Tao, L. Z.; Britt, R. D. Serine is the molecular source of the NH(CH2)(2) bridgehead moiety of the in vitro assembled FeFe hydrogenase H-cluster. *Chemical Science* **2020**, *11*, 1241−1247.

(41) Dinis, P.; Suess, D. L. M.; Fox, S. J.; Harmer, J. E.; Driesener, R. C.; De La Paz, L.; Swartz, J. R.; Essex, J. W.; Britt, R. D.; Roach, P. L. X-ray crystallographic and EPR spectroscopic analysis of HydG, a maturase in FeFe -hydrogenase H-cluster assembly. *Proc. Natl. Acad. Sci. U. S. A.* **2015**, *112*, 1362−1367.

(42) Nicolet, Y.; Zeppieri, L.; Amara, P.; Fontecilla-Camps, J. C. Crystal structure of tryptophan lyase (Nosl): Evidence for radical formation at the amino group of tryptophan. *Angew. Chem., Int. Ed.* **2014**, *53*, 11840−11844.

(43) Kuchenreuther, J. M.; Myers, W. K.; Stich, T. A.; George, S. J.; NejatyJahromy, Y.; Swartz, J. R.; Britt, R. D. A Radical Intermediate in Tyrosine Scission to the CO and CN- Ligands of FeFe Hydrogenase. *Science* **2013**, *342*, 472−475.

(44) Sayler, R. I.; Stich, T. A.; Joshi, S.; Cooper, N.; Shaw, J. T.; Begley, T. P.; Tantillo, D. J.; Britt, R. D. Trapping and Electron Paramagnetic Resonance Characterization of the 5 ' dAdo(center dot) Radical in a Radical S-Adenosyl Methionine Enzyme Reaction with a Non-Native Substrate. *ACS Cent. Sci.* **2019**, *5*, 1777−1785.

(45) Chen, N.; Rao, G.; Britt, R. D.; Wang, L.-P. Quantum Chemical Study of a Radical Relay Mechanism for the HydG-Catalyzed Synthesis of a Fe(II)(CO)$_2$(CN)cysteine Precursor to the H-Cluster of [FeFe] Hydrogenase. *Biochemistry* **2021**, *60*, 3016−3026.

(46) Nicolet, Y.; Pagnier, A.; Zeppieri, L.; Martin, L.; Amara, P.; Fontecilla-Camps, J. C. Crystal Structure of HydG from Carboxydothermus hydrogenoformans: A Trifunctional FeFe -Hydrogenase Maturase. *ChemBioChem* **2015**, *16*, 397−402.

(47) Pagnier, A.; Martin, L.; Zeppieri, L.; Nicolet, Y.; Fontecilla-Camps, J. C. CO and CN- syntheses by FeFe -hydrogenase maturase HydG are catalytically differentiated events. *Proc. Natl. Acad. Sci. U. S. A.* **2016**, *113*, 104−109.

(48) Shepard, E. M.; Impano, S.; Duffus, B. R.; Pagnier, A.; Duschene, K. S.; Betz, J. N.; Byer, A. S.; Galambas, A.; McDaniel, E. C.; Watts, H.; McGlynn, S. E.; Peters, J. W.; Broderick, W. E.; Broderick, J. B. HydG, the "Dangler" Fe, and Catalytic Production of Free CO and CN: Implications for [FeFe]-Hydrogenase Maturation. *Dalton Trans* **2021**, *50*, 10405−10422.

(49) Suess, D. L. M.; Pham, C. C.; Burstel, I.; Swartz, J. R.; Cramer, S. P.; Britt, R. D. The Radical SAM Enzyme HydG Requires Cysteine and a Dangler Iron for Generating an Organometallic Precursor to the FeFe -Hydrogenase H-Cluster. *J. Am. Chem. Soc.* **2016**, *138*, 1146−1149.

(50) Rao, G. D.; Tao, L. Z.; Suess, D. L. M.; Britt, R. D. A 4Fe-4S-Fe(CO)(CN)-L-cysteine intermediate is the first organometallic precursor in FeFe hydrogenase H-cluster bioassembly. *Nat. Chem.* **2018**, *10*, 555−560.

(51) Telser, J.; Smith, E. T.; Adams, M. W. W.; Conover, R. C.; Johnson, M. K.; Hoffman, B. M. Cyanide binding to the novel 4Fe ferredoxin from Pyrococcus-furiosus - investigation by EPR and ENDOR spectroscopy. *J. Am. Chem. Soc.* **1995**, *117*, 5133−5140.

(52) Britt, R. D.; Rauchfuss, T. B. Biosynthesis of the [FeFe] hydrogenase H-cluster via a synthetic [Fe(II)(CN)-(CO)$_2$(cysteinate)]$^-$ complex. *Dalton Trans* **2021**, *50*, 12386−12391.

(53) Tao, L.; Pattenaude, S. A.; Joshi, S.; Begley, T. P.; Rauchfuss, T. B.; Britt, R. D. Radical SAM Enzyme HydE Generates Adenosylated Fe(I) Intermediates En Route to the [FeFe]-Hydrogenase Catalytic H-Cluster. *J. Am. Chem. Soc.* **2020**, *142*, 10841−10848.

(54) Rohac, R.; Martin, L.; Liu, L.; Basu, D.; Tao, L.; Britt, R. D.; Rauchfuss, T. B.; Nicolet, Y. Crystal Structure of the [FeFe]-Hydrogenase Maturase HydE Bound to Complex-B. *J. Am. Chem. Soc.* **2021**, *143*, 8499−8508.

(55) Peters, J. W.; Lanzilotta, W. N.; Lemon, B. J.; Seefeldt, L. C. X-ray crystal structure of the Fe-only hydrogenase (Cpl) from Clostridium pasteurianum to 1.8 angstrom resolution. *Science* **1998**, *282*, 1853−1858.

(56) Lemon, B. J.; Peters, J. W. Binding of exogenously added carbon monoxide at the active site of the iron-only hydrogenase (CpI) from Clostridium pasteurianum. *Biochemistry* **1999**, *38*, 12969−12973.

(57) Nicolet, Y.; de Lacey, A. L.; Vernede, X.; Fernandez, V. M.; Hatchikian, E. C.; Fontecilla-Camps, J. C. Crystallographic and FTIR spectroscopic evidence of changes in Fe coordination upon reduction of the active site of the Fe-only hydrogenase from Desulfovibrio desulfuricans. *J. Am. Chem. Soc.* **2001**, *123*, 1596−1601.

(58) Rohac, R.; Amara, P.; Benjdia, A.; Martin, L.; Ruffie, P.; Favier, A.; Berteau, O.; Mouesca, J. M.; Fontecilla-Camps, J. C.; Nicolet, Y. Carbon-sulfur bond-forming reaction catalysed by the radical SAM enzyme HydE. *Nat. Chem.* **2016**, *8*, 491−500.

(59) Sensi, M.; Baffert, C.; Fourmond, V.; de Gioia, L.; Bertini, L.; Léger, C. Photochemistry and photoinhibition of the H-cluster of FeFe hydrogenases. *Sustainable Energy Fuels* **2021**, *5*, 4248−4260.